Chapter 2
Improved Störmer–Verlet Formulae with Applications

The Störmer–Verlet formula is a popular numerical integration method which has played an important role in the numerical simulation of differential equations. In this chapter, we analyse two improved multi-frequency Störmer–Verlet formulae with four applications, including time-independent Schrödinger equations, wave equations, orbital problems and the problem of Fermi, Pasta and Ulam. Stability and phase properties of the two improved Störmer–Verlet formulae are analysed. In order to derive the first improved multi-frequency Störmer–Verlet formula, the symplectic conditions for the one-stage explicit multi-frequency ARKN method are investigated in detail. Moreover, the coupled conditions for explicit symplectic and symmetric multi-frequency ERKN integrators are presented.

2.1 Motivation

A good numerical integrator should meet different requirements of the governing differential equation describing physical phenomena of the universe. For a differential equation with a particular structure, it is natural to require numerical algorithms to adapt to the structure of the problem and to preserve as much as possible the intrinsic properties of the true solution to the problem. A good theoretical foundation of structure-preserving algorithms for ordinary differential equations can be found in Feng et al. [8], Hairer et al. [19] and references contained therein. The time-independent Schrödinger equation is frequently encountered and is one of the basic equations of quantum mechanics. In fact, solutions of the time-independent Schrödinger equation are required in the study of atomic and molecular structure, molecular dynamics and quantum chemistry. Many numerical methods have been proposed to solve this type of Schrödinger equation. Readers are referred to [38, 48, 50] for example. In applied science and engineering, the wave equation is an important second-order partial differential equation for the description of waves. Examples of waves in physics are sound waves, light waves and water waves. It also

X. Wu et al., *Structure-Preserving Algorithms for Oscillatory Differential Equations II*, DOI 10.1007/978-3-662-48156-1_2

arises in fields like electromagnetics and fluid dynamics. The numerical treatment of wave equations is fundamental for understanding non-linear phenomena. Besides, orbital problems also constitute a very important category of differential equations in scientific computing. For an orbital problem that arises in the analysis of the motion of spacecraft, asteroids, comets, and natural or man-made satellites, it is important to maintain the accuracy of a numerical integration to a high degree of accuracy. In recent years, numerical studies of non-linear effects in physical systems have received much attention. The Fermi–Pasta–Ulam problem [9] is an important model for simulating the physics of non-linear phenomena, which reveals highly unexpected dynamical behaviour. All of the problems described above can be expressed using the following multi-frequency oscillatory second-order initial value problem:

$$\begin{cases} y'' + My = f(t, y), & t \in [t_0, t_{\text{end}}], \\ y(t_0) = y_0, \quad y'(t_0) = y_0', \end{cases} \tag{2.1}$$

where $M \in \mathbb{R}^{d\times d}$ and $f : \mathbb{R} \times \mathbb{R}^d \to \mathbb{R}^d$, $y_0 \in \mathbb{R}^d$, $y_0' \in \mathbb{R}^d$. Problems in the form (2.1) also arise in mechanics, theoretical physics, quantum dynamics, molecular biology, etc. In fact, by applying the shooting method to the one-dimensional time-independent Schrödinger equation, the boundary value problem can be converted into an initial value problem of the form (2.1). The spatial semi-discretization of a wave equation with the method of lines is an important source for (2.1). Furthermore, some orbital problems and the Fermi–Pasta–Ulam problem can also be expressed by (2.1).

If M is a symmetric and positive semi-definite matrix and $f(t, y) = -\nabla U(y)$, then with the new variables $q = y$ and $p = y'$ the system (2.1) is simply the following multi-frequency and multidimensional oscillatory Hamiltonian system

$$\begin{cases} p'(t) = -\nabla_q H(p, q), & p(t_0) = p_0 = y_0', \\ q'(t) = \nabla_p H(p, q), & q(t_0) = q_0 = y_0, \end{cases} \tag{2.2}$$

with the Hamiltonian

$$H(p, q) = \frac{1}{2} p^{\mathsf{T}} p + \frac{1}{2} q^{\mathsf{T}} M q + U(q),$$

(see Cohen et al. [5], for example). In essence, a large number of mechanical systems with a partitioned Hamiltonian function fit this pattern. Some useful approaches to constructing Runge-Kutta-Nyström (RKN) type methods for the system (2.1) have been proposed (see, e.g. [11–14, 16, 23, 40, 51]). Meanwhile, symplectic methods for the Hamiltonian system (2.2) have been developed, and readers are referred to [3, 7, 20, 34, 35, 37, 43, 44, 59] for some examples on this topic. Wu et al. [63] presented the general multi-frequency and multidimensional ARKN methods (RKN methods adapted to the system (2.1)) and derived the corresponding order conditions

based on the B-series theory. Some concrete multi-frequency and multidimensional ARKN methods are obtained in [56]. Furthermore, Wu et al. [61] formulated a standard form of the multi-frequency and multidimensional ERKN methods (extended RKN methods) for the oscillatory system (2.1) and derived the corresponding order conditions using B-series theory based on the set of ERKN trees (tri-coloured trees). Following this research, two-step ERKN methods and energy-preserving integrators are studied for the oscillatory system (2.1). Readers are referred to [28, 29, 53, 57, 62].

On the other hand, the Störmer–Verlet scheme is a classical technique for the system of second-order differential equations

$$\begin{cases} y''(t) = g\big(t, y(t)\big), \qquad t \in [t_0, t_{\text{end}}], \\ y(t_0) = y_0, \quad y'(t_0) = y'_0. \end{cases} \tag{2.3}$$

Störmer [42] used higher-order variants for numerical computations of the motion of ionized particles [42], and Verlet (1967) [49] proposed this method for computing problems in molecular dynamics. This method became known as the Störmer–Verlet method and readers are referred to [17] for a survey of this method. The Störmer–Verlet method has become by far the most widely used numerical scheme in this respect. Further examples and references can be found in [18, 30, 46] and references contained therein. Applying the Störmer–Verlet formula to (2.3) gives

$$\begin{cases} Y_1 = y_n + \dfrac{h}{2} y'_n, \\ y_{n+1} = y_n + h y'_n + \dfrac{h^2}{2} g(t_n + \dfrac{1}{2}h, Y_1), \\ y'_{n+1} = y'_n + h g(t_n + \dfrac{1}{2}h, Y_1). \end{cases} \tag{2.4}$$

The Störmer–Verlet formula (2.4) could also be applied directly to the system (2.1) providing it is rewritten in the form

$$y''(t) = f(t, y(t)) - My(t) \triangleq g(t, y(t)).$$

However, this form does not take account of the specific structure of the oscillatory system (2.1) generated by the linear term My. Both the multi-frequency ARKN scheme and ERKN scheme are formulated from the formula of the integral equations (see Theorem 1.1 in Chap. 1) adapted to the system (2.1). They are expected to have better numerical behaviour than the classical Störmer–Verlet formula. The key point here is that each new multi-frequency and multidimensional Störmer–Verlet formula utilizes a combination of existing trigonometric integrators and symplectic schemes.

2.2 Two Improved Störmer–Verlet Formulae

Two improved multi-frequency and multidimensional Störmer–Verlet formulae for the oscillatory system (2.1) are presented below.

2.2.1 Improved Störmer–Verlet Formula 1

The first improved Störmer–Verlet formula is based on the multi-frequency and multidimensional ARKN schemes and the corresponding symplectic conditions. Taking advantage of the specific structure of (2.1) introduced by the linear term My and revising the updates of RKN methods, we obtain s-stage multi-frequency and multidimensional ARKN methods for (2.1) (see [63])

$$\begin{cases} Y_i = y_n + c_i h y_n' + h^2 \sum_{j=1}^{s} \bar{a}_{ij} \big(f(t_n + c_j h, Y_j) - M Y_j \big), \quad i = 1, 2, \ldots, s, \\ y_{n+1} = \phi_0(V) y_n + \phi_1(V) h y_n' + h^2 \sum_{i=1}^{s} \bar{b}_i(V) f(t_n + c_i h, Y_i), \\ h y_{n+1}' = -V \phi_1(V) y_n + \phi_0(V) h y_n' + h^2 \sum_{i=1}^{s} b_i(V) f(t_n + c_i h, Y_i), \end{cases} \tag{2.5}$$

where h is the stepsize, $\bar{a}_{ij}$ for $i, j = 1, 2, \ldots, s$ are real constants, $b_i(V)$ and $\bar{b}_i(V)$ for $i = 1, 2, \ldots, s$ are matrix-valued functions of $V = h^2 M$, $\phi_0(V)$ and $\phi_1(V)$ are given by (1.7). In order to derive an improved Störmer–Verlet formula for (2.1), the one-stage explicit multi-frequency and multidimensional ARKN method of the form below is considered:

$$\begin{cases} Y_1 & = y_n + c_1 h y_n', \\ y_{n+1} & = \phi_0(V) y_n + \phi_1(V) h y_n' + h^2 \bar{b}_1(V) f(t_n + c_1 h, Y_1), \\ h y_{n+1}' & = -V \phi_1(V) y_n + \phi_0(V) h y_n' + h^2 b_1(V) f(t_n + c_1 h, Y_1). \end{cases} \tag{2.6}$$

The symplectic conditions for the one-stage explicit multi-frequency and multidimensional ARKN method (2.6) are examined below.

Theorem 2.1 *Suppose that M is symmetric and positive semi-definite and $f(y) = -\nabla U(y)$ is the negative gradient of the function $U(y)$ with continuous second derivatives with respect to y. If the coefficients of a multi-frequency and multidimensional ARKN method (2.6) satisfy*

$$b_1(V)\phi_0(V) + \bar{b}_1(V) V \phi_1(V) = d_1 I, \ d_1 \in \mathbb{R}, \tag{2.7}$$

$$\bar{b}_1(V)(\phi_0(V) + c_1 V \phi_1(V)) = b_1(V)(\phi_1(V) - c_1 \phi_0(V)), \tag{2.8}$$

where I is the identity matrix, then the method is symplectic.

Proof Following the approach used in [37], we will adopt exterior forms.

First consider the special case where M is a diagonal matrix with nonnegative entries: $M = \mathrm{diag}(m_{11}, m_{22}, \ldots, m_{dd})$. Accordingly, $\phi_0(V)$, $\phi_1(V)$, $b_1(V)$ and $\bar{b}_1(V)$ are all diagonal matrices. Denote $f_1 = f(Y_1)$. Then the ARKN scheme (2.6) becomes

$$\begin{cases} Y_1^J = y_n^J + c_1 h y_n'^J, \\ y_{n+1}^J = \phi_0(h^2 m_{JJ}) y_n^J + \phi_1(h^2 m_{JJ}) h y_n'^J + h^2 \bar{b}_1(h^2 m_{JJ}) f_1^J, \\ y_{n+1}'^J = -h m_{JJ} \phi_1(h^2 m_{JJ}) y_n^J + \phi_0(h^2 m_{JJ}) y_n'^J + h b_1(h^2 m_{JJ}) f_1^J, \end{cases} \tag{2.9}$$

where the superscript J ($J = 1, 2, \ldots, d$) denotes the Jth component of a vector. In terms of the above notations and the Hamiltonian system (2.2), symplecticity of the method (2.6) is identical to

$$\sum_{J=1}^{d} \mathrm{d}y_{n+1}^J \wedge \mathrm{d}y_{n+1}'^J = \sum_{J=1}^{d} \mathrm{d}y_n^J \wedge \mathrm{d}y_n'^J.$$

To show this equality, it is required to compute

$$\begin{aligned} \mathrm{d}y_{n+1}^J \wedge \mathrm{d}y_{n+1}'^J &= [\phi_0^2(h^2 m_{JJ}) + h^2 m_{JJ} \phi_1^2(h^2 m_{JJ})] \mathrm{d}y_n^J \wedge \mathrm{d}y_n'^J \\ &\quad + h[b_1(h^2 m_{JJ}) \phi_0(h^2 m_{JJ}) + \bar{b}_1(h^2 m_{JJ}) h^2 m_{JJ} \phi_1(h^2 m_{JJ})] \mathrm{d}y_n^J \wedge \mathrm{d}f_1^J \\ &\quad + h^2[b_1(h^2 m_{JJ}) \phi_1(h^2 m_{JJ}) - \bar{b}_1(h^2 m_{JJ}) \phi_0(h^2 m_{JJ})] \mathrm{d}y_n'^J \wedge \mathrm{d}f_1^J. \end{aligned}$$

It follows from the definition (1.7) that

$$\begin{aligned} \phi_0^2(h^2 m_{JJ}) + h^2 m_{JJ} \phi_1^2(h^2 m_{JJ}) &= \cos^2(h\sqrt{m_{JJ}}) + h^2 m_{JJ} \Big(\frac{\sin(h\sqrt{m_{JJ}})}{h\sqrt{m_{JJ}}} \Big)^2 \\ &= \cos^2(h\sqrt{m_{JJ}}) + \sin^2(h\sqrt{m_{JJ}}) = 1. \end{aligned}$$

Thus,

$$\begin{aligned} \mathrm{d}y_{n+1}^J \wedge \mathrm{d}y_{n+1}'^J &= \mathrm{d}y_n^J \wedge \mathrm{d}y_n'^J \\ &\quad + h[b_1(h^2 m_{JJ}) \phi_0(h^2 m_{JJ}) + \bar{b}_1(h^2 m_{JJ}) h^2 m_{JJ} \phi_1(h^2 m_{JJ})] \mathrm{d}y_n^J \wedge \mathrm{d}f_1^J \\ &\quad + h^2[b_1(h^2 m_{JJ}) \phi_1(h^2 m_{JJ}) - \bar{b}_1(h^2 m_{JJ}) \phi_0(h^2 m_{JJ})] \mathrm{d}y_n'^J \wedge \mathrm{d}f_1^J. \end{aligned} \tag{2.10}$$

Differentiating the first formula of (2.9) yields

$$\mathrm{d}y_n^J = \mathrm{d}Y_1^J - h c_1 \mathrm{d}y_n'^J.$$

Then, one obtains

$$\mathrm{d}y_n^J \wedge \mathrm{d}f_1^J = \mathrm{d}Y_1^J \wedge \mathrm{d}f_1^J - hc_1\mathrm{d}y_n'^J \wedge \mathrm{d}f_1^J.$$

Inserting this formula into (2.10) gives

$$\begin{aligned}\mathrm{d}y_{n+1}^J \wedge \mathrm{d}y_{n+1}'^J &= \mathrm{d}y_n^J \wedge \mathrm{d}y_n'^J \\ &+ h[b_1(h^2m_{JJ})\phi_0(h^2m_{JJ}) + \bar{b}_1(h^2m_{JJ})h^2m_{JJ}\phi_1(h^2m_{JJ})]\mathrm{d}Y_1^J \wedge \mathrm{d}f_1^J \\ &+ h^2[b_1(h^2m_{JJ})\phi_1(h^2m_{JJ}) - \bar{b}_1(h^2m_{JJ})\phi_0(h^2m_{JJ}) \\ &- c_1b_1(h^2m_{JJ})\phi_0(h^2m_{JJ}) - c_1\bar{b}_1(h^2m_{JJ})h^2m_{JJ}\phi_1(h^2m_{JJ})]\mathrm{d}y_n'^J \wedge \mathrm{d}f_1^J.\end{aligned} \tag{2.11}$$

Summing over all J yields

$$\begin{aligned}&\sum_{J=1}^{d}\mathrm{d}y_{n+1}^J \wedge \mathrm{d}y_{n+1}'^J = \sum_{J=1}^{d}\mathrm{d}y_n^J \wedge \mathrm{d}y_n'^J \\ &+ h\sum_{J=1}^{d}[b_1(h^2m_{JJ})\phi_0(h^2m_{JJ}) + \bar{b}_1(h^2m_{JJ})h^2m_{JJ}\phi_1(h^2m_{JJ})]\mathrm{d}Y_1^J \wedge \mathrm{d}f_1^J \\ &+ h^2\sum_{J=1}^{d}[b_1(h^2m_{JJ})\phi_1(h^2m_{JJ}) - \bar{b}_1(h^2m_{JJ})\phi_0(h^2m_{JJ}) \\ &- c_1b_1(h^2m_{JJ})\phi_0(h^2m_{JJ}) - c_1\bar{b}_1(h^2m_{JJ})h^2m_{JJ}\phi_1(h^2m_{JJ})]\mathrm{d}y_n'^J \wedge \mathrm{d}f_1^J.\end{aligned} \tag{2.12}$$

By (2.7) and $f(y) = -\nabla_y U(y)$, where U has continuous second derivatives with respect to y, one obtains

$$\begin{aligned}&\sum_{J=1}^{d}[b_1(h^2m_{JJ})\phi_0(h^2m_{JJ}) + \bar{b}_1(h^2m_{JJ})h^2m_{JJ}\phi_1(h^2m_{JJ})]\mathrm{d}Y_1^J \wedge \mathrm{d}f_1^J \\ &= \sum_{J=1}^{d} d_1\mathrm{d}Y_1^J \wedge \mathrm{d}f_1^J = -d_1\sum_{J,I=1}^{d}(\frac{\partial f^J}{\partial y^I}\mathrm{d}Y_1^I) \wedge \mathrm{d}Y_1^J \\ &= -d_1\sum_{J,I=1}^{d}(-\frac{\partial^2 U}{\partial y^J\partial y^I})\mathrm{d}Y_1^I \wedge \mathrm{d}Y_1^J = 0.\end{aligned}$$

According to (2.8), the last term of (2.12) is equal to zero. Therefore,

$$\sum_{J=1}^{d}\mathrm{d}y_{n+1}^J \wedge \mathrm{d}y_{n+1}'^J = \sum_{J=1}^{d}\mathrm{d}y_n^J \wedge \mathrm{d}y_n'^J.$$

For the general case, where M is a symmetric and positive semi-definite matrix, the decomposition of M may be written as follows

$$M = P^{\mathsf{T}}W^2P = \Omega_0^2 \text{ with } \Omega_0 = P^{\mathsf{T}}WP,$$

where P is an orthogonal matrix and W is a diagonal matrix with nonnegative diagonal entries which are the square roots of the eigenvalues of M. Using the variable substitution $z(t) = Py(t)$ the system (2.1) is equivalent to

$$\begin{cases} z'' + W^2 z = Pf(P^{\intercal} z), \\ z(t_0) = z_0 = Py_0, \\ z'(t_0) = z'_0 = Py'_0. \end{cases} \tag{2.13}$$

Then symplectic integrators for the diagonal matrix M with nonnegative entries can be applied to the transformed system. Moreover, the methods are invariant under linear transformations. This means that the ARKN method (2.6) with symplecticity conditions (2.7) and (2.8) can be applied to systems with M a symmetric and positive semi-definite matrix.

It may be concluded that the ARKN method (2.6), satisfying symplectic conditions (2.7) and (2.8), is a symplectic integrator for the system (2.1) with symmetric and positive semi-definite M. □

With Theorem 2.1, a one-stage explicit symplectic multi-frequency and multi-dimensional ARKN method can be derived. Regarding c_1, d_1 as parameters, the Eqs. (2.7) and (2.8) may be rewritten as

$$\begin{cases} b_1(V) = d_1\big(\phi_0(V) + c_1 V\phi_1(V)\big), \\ \bar{b}_1(V) = d_1\big(\phi_1(V) - c_1\phi_0(V)\big). \end{cases} \tag{2.14}$$

The choice of $d_1 = 1$ and $c_1 = \dfrac{1}{2}$ gives the following symplectic multi-frequency and multidimensional ARKN formula:

$$\begin{cases} Y_1 = y_n + \dfrac{1}{2}hy'_n, \\ y_{n+1} = \phi_0(V)y_n + \phi_1(V)hy'_n + h^2\big(\phi_1(V) - \dfrac{1}{2}\phi_0(V)\big)f(t_n + \dfrac{1}{2}h, Y_1), \\ hy'_{n+1} = -V\phi_1(V)y_n + \phi_0(V)hy'_n + h^2\big(\phi_0(V) + \dfrac{1}{2}V\phi_1(V)\big)f(t_n + \dfrac{1}{2}h, Y_1). \end{cases} \tag{2.15}$$

It can be verified that this formula is of order two from the order conditions of ARKN methods in Wu et al. [63]. This improved Störmer–Verlet formula (2.15) is denoted by ISV1.

2.2.2 *Improved Störmer–Verlet Formula 2*

The second improved Störmer–Verlet formula is based on the multi-frequency and multidimensional ERKN integrators and the corresponding symplectic conditions.

Taking advantage of the specific structure given by the linear term My of (2.1), and revising not only the updates but also the internal stages of classical RKN methods leads to the so-called multi-frequency and multidimensional ERKN integrators.

Definition 2.1 An s-stage multi-frequency and multidimensional ERKN integrator for the system (2.1) is defined as in [61]:

$$\begin{cases} Y_i = \phi_0(c_i^2V)y_n + c_i\phi_1(c_i^2V)hy_n' + h^2\sum\limits_{j=1}^{s}\bar{a}_{ij}(V)f(t_n + c_jh, Y_j), \quad i = 1, 2, \ldots, s, \\ y_{n+1} = \phi_0(V)y_n + \phi_1(V)hy_n' + h^2\sum\limits_{i=1}^{s}\bar{b}_i(V)f(t_n + c_ih, Y_i), \\ hy_{n+1}' = -V\phi_1(V)y_n + \phi_0(V)hy_n' + h^2\sum\limits_{i=1}^{s}b_i(V)f(t_n + c_ih, Y_i), \end{cases} \tag{2.16}$$

where c_i for $i = 1, 2, \ldots, s$, are real constants, $b_i(V)$, $\bar{b}_i(V)$ and $\bar{a}_{ij}(V)$ for $i, j = 1, 2, \ldots, s$, are matrix-valued functions of $V = h^2M$.

Our attention is only focused on the one-stage explicit multi-frequency and multidimensional ERKN method as given below:

$$\begin{cases} Y_1 = \phi_0(c_1^2V)y_n + c_1\phi_1(c_1^2V)hy_n', \\ y_{n+1} = \phi_0(V)y_n + \phi_1(V)hy_n' + h^2\bar{b}_1(V)f(t_n + c_1h, Y_1), \\ hy_{n+1}' = -V\phi_1(V)y_n + \phi_0(V)hy_n' + h^2b_1(V)f(t_n + c_1h, Y_1). \end{cases} \tag{2.17}$$

The symplectic conditions for the one-stage explicit multi-frequency and multidimensional ERKN method (2.17) are presented by the following theorem.

Theorem 2.2 *Under the conditions of Theorem 2.1, the one-stage explicit multi-frequency and multidimensional ERKN method (2.17) is symplectic if its coefficients satisfy*

$$\begin{cases} b_1(V)\phi_0(V) + \bar{b}_1(V)V\phi_1(V) = d_1\phi_0(c_1^2V), \ d_1 \in \mathbb{R}, \\ \bar{b}_1(V)\big(\phi_0(V) + c_1V\phi_1(V)\phi_0^{-1}(c_1^2V)\phi_1(c_1^2V)\big) \\ \quad = b_1(V)\big(\phi_1(V) - c_1\phi_0(V)\phi_0^{-1}(c_1^2V)\phi_1(c_1^2V)\big). \end{cases} \tag{2.18}$$

Proof It follows from the Theorem 3.1 in Wu et al. [59]. □

The one-stage explicit symplectic multi-frequency and multidimensional ERKN method (2.17) can be obtained by solving the equations in (2.18) with c_1, d_1 as parameters. This leads to

$$\begin{cases} b_1(V) = d_1\big(\phi_0(V)\phi_0(c_1^2V) + c_1V\phi_1(V)\phi_1(c_1^2V)\big), \\ \bar{b}_1(V) = d_1\big(\phi_1(V)\phi_0(c_1^2V) - c_1V\phi_0(V)\phi_1(c_1^2V)\big). \end{cases} \tag{2.19}$$

Choosing $d_1 = 1$ and $c_1 = \frac{1}{2}$ yields the following symplectic multidimensional ERKN formula

$$\begin{cases} Y_1 = \phi_0(\frac{V}{4})y_n + \frac{1}{2}\phi_1(\frac{V}{4})hy'_n, \\ y_{n+1} = \phi_0(V)y_n + \phi_1(V)hy'_n + \frac{h^2}{2}\phi_1(\frac{V}{4})f(t_n + \frac{1}{2}h, Y_1), \\ hy'_{n+1} = -V\phi_1(V)y_n + \phi_0(V)hy'_n + h^2\phi_0(\frac{V}{4})f(t_n + \frac{1}{2}h, Y_1), \end{cases} \tag{2.20}$$

which is denoted by ISV2. From the order conditions of multidimensional ERKN methods presented in Wu et al. [61], this formula can be verified to be of order two. Moreover, this formula is symplectic and symmetric.

Note that the formula ISV1 amends the updates, and the formula ISV2 modifies both the internal stages and the updates to adapt them to the qualitative behaviour of the true solution. Therefore, the two formulae ISV1 and ISV2 are derived by making use of the specific structure of the Eq. (2.1) introduced by the linear term My. An important observation is that as $M \to \mathbf{0}_{d\times d}$, both formulae ISV1 and ISV2 reduce to the well-known classical Störmer–Verlet formula (2.4). In this sense the formulae ISV1 and ISV2 are extensions of the classical Störmer–Verlet formula (2.4).

2.3 Stability and Phase Properties

It is important to analyse the stability and phase properties of an oscillatory integrator, including dispersion and dissipation (see, e.g. [47]) of the numerical method. This section examines the stability and phase properties of the new formulae ISV1 and ISV2.

The following test equation is given in [47, 55] for stability analysis of the new formulae:

$$y''(t) + \omega^2 y(t) = -\varepsilon y(t) \text{ with } \omega^2 + \varepsilon > 0, \tag{2.21}$$

where ω represents an estimation of the dominant frequency λ and $\varepsilon = \lambda^2 - \omega^2$ is the error of the estimation.

Applying the formula ISV1 determined by (2.15) to (2.21) yields

$$\begin{cases} Y_1 = y_n + \frac{1}{2}hy'_n, \quad z = \varepsilon h^2, \quad V = h^2\omega^2, \\ y_{n+1} = \phi_0(V)y_n + \phi_1(V)hy'_n - z\big(\phi_1(V) - \frac{1}{2}\phi_0(V)\big)Y_1, \\ hy'_{n+1} = -V\phi_1(V)y_n + \phi_0(V)hy'_n - z\big(\phi_0(V) + \frac{1}{2}V\phi_1(V)\big)Y_1. \end{cases} \tag{2.22}$$

It follows from (2.22) that

$$\begin{pmatrix} y_{n+1} \\ hy'_{n+1} \end{pmatrix} = S_1(V,z) \begin{pmatrix} y_n \\ hy'_n \end{pmatrix},$$

where the stability matrix $S_1(V,z)$ of the formula ISV1 is given by

$$S_1(V,z) = \begin{pmatrix} \phi_0(V) - z\big(\phi_1(V) - \frac{1}{2}\phi_0(V)\big) & \phi_1(V) - \frac{1}{2}z\big(\phi_1(V) - \frac{1}{2}\phi_0(V)\big) \\ -V\phi_1(V) - z\big(\phi_0(V) + \frac{1}{2}V\phi_1(V)\big) & \phi_0(V) - \frac{1}{2}z\big(\phi_0(V) + \frac{1}{2}V\phi_1(V)\big) \end{pmatrix}.$$

Likewise, applying the formula ISV2 determined by (2.20) to (2.21) yields

$$\begin{cases} Y_1 = \phi_0\big(\frac{V}{4}\big)y_n + \frac{1}{2}\phi_1\big(\frac{V}{4}\big)hy'_n, \qquad z = \varepsilon h^2, \qquad V = h^2\omega^2, \\ y_{n+1} = \phi_0(V)y_n + \phi_1(V)hy'_n - \frac{z}{2}\phi_1\big(\frac{V}{4}\big)Y_1, \\ hy'_{n+1} = -V\phi_1(V)y_n + \phi_0(V)hy'_n - z\phi_0\big(\frac{V}{4}\big)Y_1. \end{cases}$$

Thus we have

$$\begin{pmatrix} y_{n+1} \\ hy'_{n+1} \end{pmatrix} = S_2(V,z) \begin{pmatrix} y_n \\ hy'_n \end{pmatrix},$$

where the stability matrix $S_2(V,z)$ of the formula ISV2 is given by

$$S_2(V,z) = \begin{pmatrix} \phi_0(V) - \frac{z}{2}\phi_1\big(\frac{1}{4}V\big)\phi_0\big(\frac{1}{4}V\big) & \phi_1(V) - \frac{z}{2}\phi_1\big(\frac{1}{4}V\big)\Big(\frac{1}{2}\phi_1\big(\frac{1}{4}V\big)\Big) \\ -V\phi_1(V) - z\phi_0\big(\frac{1}{4}V\big)\phi_0\big(\frac{1}{4}V\big) & \phi_0(V) - z\phi_0\big(\frac{1}{4}V\big)\Big(\frac{1}{2}\phi_1\big(\frac{1}{4}V\big)\Big) \end{pmatrix}.$$

The spectral radii $\rho\big(S_1(V,z)\big)$ and $\rho\big(S_2(V,z)\big)$ represent the stability of formulae ISV1 and ISV2, respectively. Since each stability matrix $S(V,z)$ depends on the variables V and z, geometrically, the characterization of stability becomes a two-dimensional region in the (V,z)-plane. Accordingly, the following definition of stability for the two new formulae can be used.

Definition 2.2 For the stability matrix $S(V,z)$ of each formula, $S_s = \{(V,z)|\ V > 0\ \textit{and}\ \rho(S) < 1\}$ is called the stability region of the formula. Accordingly, $S_p = \{(V,z)|\ V > 0,\ \rho(S) = 1\ \textit{and}\ \mathrm{tr}(S)^2 < 4\det(S)\}$ is called the *periodicity region of the formula*.

The stability regions of the formulae ISV1 and ISV2 are shown in Fig. 2.1.

Definition 2.3 The quantities

$$\phi(H) = H - \arccos\Big(\frac{\mathrm{tr}(S)}{2\sqrt{\det(S)}}\Big), \quad d(H) = 1 - \sqrt{\det(S)}$$

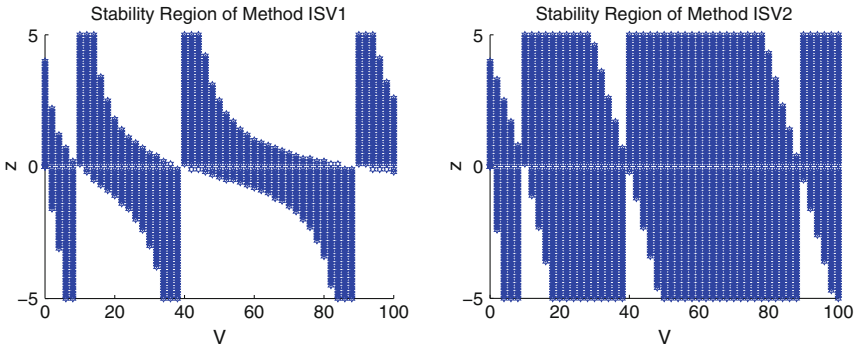

Fig. 2.1 Stability regions for the methods ISV1 (*left*) and ISV2 (*right*)

are called the dispersion error and the dissipation error of the integrator, respectively, where $H = \sqrt{V + z}$. Then, an integrator is said to be dispersive of order q and dissipative of order r, if $\phi(H) = \mathscr{O}(H^{q+1})$ and $d(H) = \mathscr{O}(H^{r+1})$, respectively. If $\phi(H) = 0$ and $d(H) = 0$, the integrator is said to be zero dispersive and zero dissipative, respectively.

With regard to the phase properties of the new formulae ISV1 and ISV2, we have

- ISV1: $\phi(H) = -\dfrac{\varepsilon(\varepsilon + 3\omega^2)H^3}{24(\varepsilon + \omega^2)^2} + \mathscr{O}(H^5)$,
- ISV2: $\phi(H) = -\dfrac{\varepsilon^2 H^3}{24(\varepsilon + \omega^2)^2} + \mathscr{O}(H^5)$.

Since the formulae ISV1 and ISV2 are both symplectic, one has $\det(S_i) = 1$ for $i = 1, 2$ and hence both the formulae ISV1 and ISV2 are zero dissipative.

2.4 Applications

In this section, four applications of the two improved Störmer–Verlet formulae are used to demonstrate their remarkable efficiency. These four types of problems are the one-dimensional time-independent Schrödinger equations, the non-linear wave equations, orbital problems and the Fermi–Pasta–Ulam problem. The numerical methods used for comparison are:

- SV: the classical Störmer–Verlet formula (2.4);
- A: the symmetric and symplectic Gautschi-type method of order two given in [13];
- B: the symmetric Gautschi-type method of order two given in [16];
- ISV1: the improved Störmer–Verlet formula given by (2.15) in this chapter;
- ISV2: the improved Störmer–Verlet formula given by (2.20) in this chapter.

2.4.1 Application 1: Time-Independent Schrödinger Equations

The time-independent Schrödinger equation is one of the basic equations of quantum mechanics. For the one-dimensional case, it may be written in the form (see, e.g. [24])

$$\frac{\mathrm{d}^2\Psi}{\mathrm{d}x^2} + 2E\Psi = 2V(x)\Psi, \tag{2.23}$$

where E is the energy eigenvalue, $V(x)$ the potential and $\Psi(x)$ the wave function. Consider the Eq. (2.23) with boundary conditions

$$\Psi(a) = 0, \ \Psi(b) = 0, \tag{2.24}$$

and use the shooting scheme in the implementation of the above methods. It is well known that the shooting method converts the boundary value problem to an initial value problem. Here, the boundary value at the end point b is transformed to an initial value $\Psi'(a)$, and the results are independent of $\Psi'(a)$ if $\Psi'(a) \neq 0$. The eigenvalue E is a parameter here and its value making $\Psi(b) = 0$ is the eigenvalue computed.

The two improved Störmer–Verlet formulae are tested against the classical Störmer–Verlet formula and the two Gautschi-type methods A and B through the following two cases.

Case 1: The harmonic oscillator
The potential of the one-dimensional harmonic oscillator is

$$V(x) = \frac{1}{2}kx^2,$$

with the interval of integration $[a, b]$ and boundary conditions $\Psi(a) = \Psi(b) = 0$. With $k = 1$ and $M = 2E$, the eigenvalues are computed as $E = 5.5$ and $E = 20.5$ using the stepsizes $h = 0.01, 0.02, 0.03, 0.04$ on the interval $[-8, 8]$. The errors between the energy eigenvalue E and that calculated by each numerical method ($ERR = |E - E_{\text{calculated}}|$) are shown in Fig. 2.2.

Case 2: Doubly anharmonic oscillator
The potential of the doubly anharmonic oscillator is

$$V(x) = \frac{1}{2}x^2 + \lambda_1 x^4 + \lambda_2 x^6.$$

The boundary conditions for this problem are $\Psi(a) = \Psi(b) = 0$. With $\lambda_1 = \lambda_2 = \frac{1}{2}$, the eigenvalues are computed as $E = 54.2225$ and $E = 145.0317$ on the interval $[-5, 5]$ using the stepsizes $h = 0.005, 0.01, 0.015, 0.02$. The results are shown in Fig. 2.3.

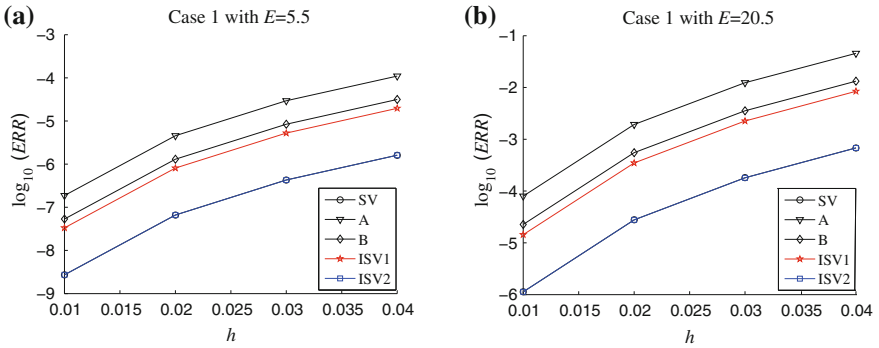

Fig. 2.2 Results for Case 1. The logarithm of the error $ERR = |E - E_{\text{calculated}}|$ against the stepsizes h

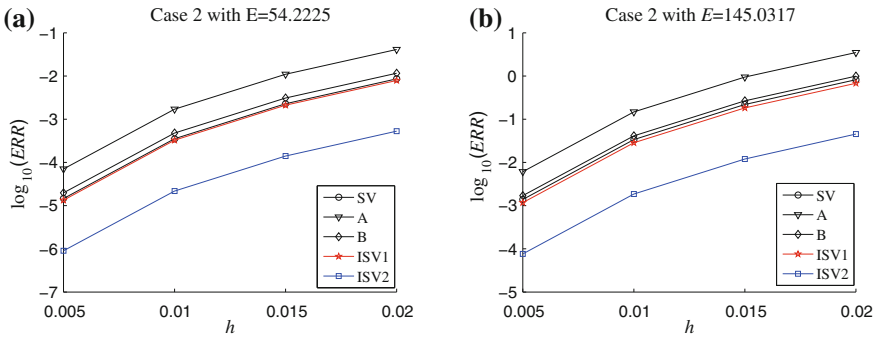

Fig. 2.3 Results for Case 2. The logarithm of the error $ERR = |E - E_{\text{calculated}}|$ against the stepsizes h

2.4.2 Application 2: Non-linear Wave Equations

For each problem in this section and the next two sections, the efficiency curves, i.e. accuracy versus the computational cost measured by the number of function evaluations required by each method, will be shown. If a problem is a Hamiltonian system, the numerical energy conservation is presented for each method. In this section, a non-linear wave equation is studied.

Problem 2.1 Consider the non-linear wave equation (see [11])

$$\begin{cases} \dfrac{\partial^2 u}{\partial t^2} - a(x)\dfrac{\partial^2 u}{\partial x^2} + 92u = f(t,x,u), \quad 0 < x < 1, \ t > 0. \\ u(0,t) = 0, \quad u(1,t) = 0, \quad u(x,0) = a(x), \quad u_t(x,0) = 0, \end{cases}$$

where

$$f(t,x,u) = u^5 - a^2(x)u^3 + \frac{a^5(x)}{4}\sin^2(20t)\cos(10t), \quad a(x) = 4x(1-x).$$

The exact solution is $u(x,t) = a(x)\cos(10t)$. The oscillatory problem represents a vibrating string with angular speed 10. A semi-discretization of the wave equation of the spatial variable by means of second-order symmetric differences yields the following second-order ordinary differential equations in time

$$\begin{cases} \dfrac{\mathrm{d}^2u_i(t)}{\mathrm{d}t^2} - a(x_i)\dfrac{u_{i+1}(t) - 2u_i(t) + u_{i-1}(t)}{\Delta x^2} + 92u_i(t) = f\big(t, x_i, u_i(t)\big), \quad 0 < t \le t_{\mathrm{end}}, \\ u_i(0) = a(x_i), \quad u_i'(0) = 0, \quad i = 1, 2, \ldots, N-1, \end{cases}$$

where $\Delta x = 1/N$ is the spatial mesh step, $x_i = i\Delta x$ and $u_i(t) \approx u(x_i, t)$. This system takes the form

$$\begin{cases} \dfrac{\mathrm{d}^2U(t)}{\mathrm{d}t^2} + MU(t) = F\big(t, U(t)\big), \quad 0 < t \le t_{\mathrm{end}}, \\ U(0) = \big(a(x_1), \ldots, a(x_{N-1})\big)^{\mathsf{T}}, \quad U'(0) = \mathbf{0}, \end{cases} \tag{2.25}$$

where $U(t) = \big(u_1(t), \ldots, u_{N-1}(t)\big)^{\mathsf{T}}$,

$$M = \frac{1}{\Delta x^2}\begin{pmatrix} 2a(x_1) & -a(x_1) & & & \\ -a(x_2) & 2a(x_2) & -a(x_2) & & \\ & \ddots & \ddots & \ddots & \\ & & -a(x_{N-2}) & 2a(x_{N-2}) & -a(x_{N-2}) \\ & & & -a(x_{N-1}) & 2a(x_{N-1}) \end{pmatrix} + 92I_{N-1},$$

and

$$F(t, U(t)) = \Big(f\big(t, x_1, u_1(t)\big), \ldots, f\big(t, x_{N-1}, u_{N-1}(t)\big)\Big)^{\mathsf{T}}.$$

Note that the matrix M is not symmetric and the system (2.25) is not a Hamiltonian system. However, (2.25) is an oscillatory system. The system is integrated on the interval $[0, 100]$ with $N = 20$ and the integration stepsizes $h = 1/(40 \times 2^j)$, $j = 0, 1, 2, 3$. Figure 2.4 shows the errors in the positions at $t_{\mathrm{end}} = 100$ versus the computational effort.

It can be observed from Fig. 2.4 that the two novel improved Störmer–Verlet formulae outperform the classical Störmer–Verlet formula and the others in terms of efficiency.

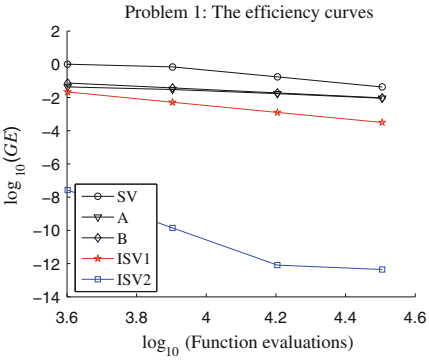

Fig. 2.4 Results for Problem 2.1. The logarithm of the global error (GE) over the integration interval against the logarithm of the number of function evaluations

2.4.3 Application 3: Orbital Problems

In this section, three orbital problems are solved using the two improved formulae ISV1 and ISV2, and the two Gautschi-type methods A in [13] and B in [16], as well as the Störmer–Verlet formula. The numerical results are shown.

Problem 2.2 Consider the Hamiltonian equation which governs the motion of an artificial satellite (see [41]) with the Hamiltonian function

$$H(q,\,p) = \frac{1}{2}p^{\mathsf{T}}p + \frac{\hbar}{4}q^{\mathsf{T}}q + \lambda\Big(\frac{(q_1q_3 + q_2q_4)^2}{r^4} - \frac{1}{12r^2}\Big),$$

where $q = (q_1, q_2, q_3, q_4)^{\mathsf{T}}$, $p = (p_1, p_2, p_3, p_4)^{\mathsf{T}}$, $r = q^{\mathsf{T}}q$, and $\hbar$ is the total energy of the elliptic motion which is defined by $\hbar = \frac{K^2-2|p_0|^2}{r_0} - V_0$ with $V_0 = -\dfrac{\lambda}{12r_0^3}$. The initial conditions are considered on an elliptic equatorial orbit as

$$q_0 = \sqrt{\frac{r_0}{2}}\Big(-1, -\frac{\sqrt{3}}{2}, -\frac{1}{2}, 0\Big)^{\mathsf{T}}, \quad p_0 = \frac{1}{2}\sqrt{K^2\frac{1+e}{2}}\Big(1, \frac{\sqrt{3}}{2}, \frac{1}{2}, 0\Big)^{\mathsf{T}}.$$

The parameters of this problem are chosen as $K^2 = 3.98601 \times 10^5$, $r_0 = 6.8 \times 10^3$, $e = 0.1$, $\lambda = \frac{3}{2}K^2J_2R^2$, $J_2 = 1.08625 \times 10^{-3}$, $R = 6.37122 \times 10^3$.

The problem is solved on the interval $[0, 100]$. The integration stepsizes are taken as $h = 2^j/300$ with $j = 2, \ldots, 5$. The numerical results are shown in Fig. 2.5a. For the global errors of Hamiltonian, the stepsize used here is $h = 1/100$ on the intervals $[0, 10^i]$, $i = 0, 1, 2, 3$. See Fig. 2.5b for the results.

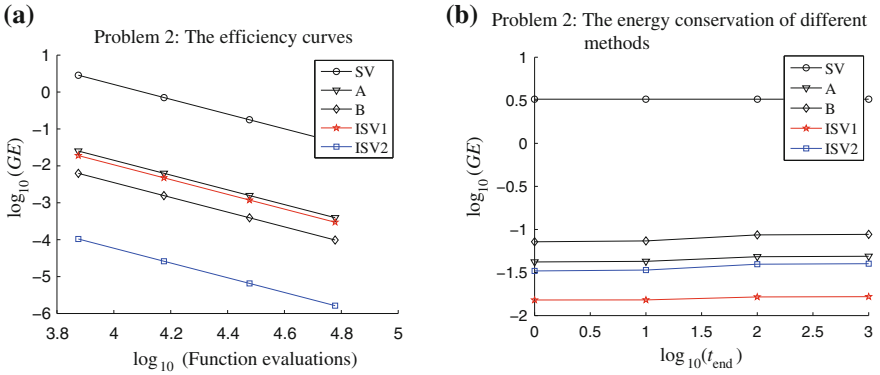

Fig. 2.5 Results for Problem 2.2. **a** The logarithm of the global error (GE) over the integration interval against the logarithm of the number of function evaluations. **b** The logarithm of the maximum global error of Hamiltonian $GEH = \max |H_n - H_0|$ against $\log_{10}(t_{\text{end}})$

Problem 2.3 Consider the orbital problem with perturbation

$$\begin{cases} q_1''(t) + q_1(t) = -\dfrac{2\varepsilon + \varepsilon^2}{r^5} q_1(t), \quad q_1(0) = 1,\ q_1'(0) = 0, \\ q_2''(t) + q_2(t) = -\dfrac{2\varepsilon + \varepsilon^2}{r^5} q_2(t), \quad q_2(0) = 0,\ q_2'(0) = 1 + \varepsilon, \end{cases}$$

where $r = \sqrt{q_1^2(t) + q_2^2(t)}$. Its analytic solution is given by

$$q_1(t) = \cos(t + \varepsilon t), \quad q_2(t) = \sin(t + \varepsilon t).$$

The problem has been solved on the interval $[0, 1000]$ with $\varepsilon = 10^{-3}$. The stepsizes are taken as $h = 1/(2^j)$ with $j = 3, \ldots, 6$. The numerical results are shown in Fig. 2.6a.

This system is a Hamiltonian system with the Hamiltonian

$$H = \frac{p_1^2 + p_2^2}{2} + \frac{q_1^2 + q_2^2}{2} - \frac{2\varepsilon + \varepsilon^2}{3(q_1^2 + q_2^2)^{\frac{3}{2}}}.$$

Accordingly, we integrate this problem with the stepsize $h = 1/8$ on the intervals $[0, 10^i]$, $i = 1, \ldots, 4$. The energy conservation of different methods is shown in Fig. 2.6b.

Problem 2.4 Consider the model for stellar orbits in a galaxy (see [25, 26])

$$\begin{cases} q_1''(t) + a^2 q_1(t) = \varepsilon q_2^2(t), & q_1(0) = 1,\ q_1'(0) = 0, \\ q_2''(t) + b^2 q_2(t) = 2\varepsilon q_1(t) q_2(t), & q_2(0) = 1,\ q_2'(0) = 0, \end{cases}$$

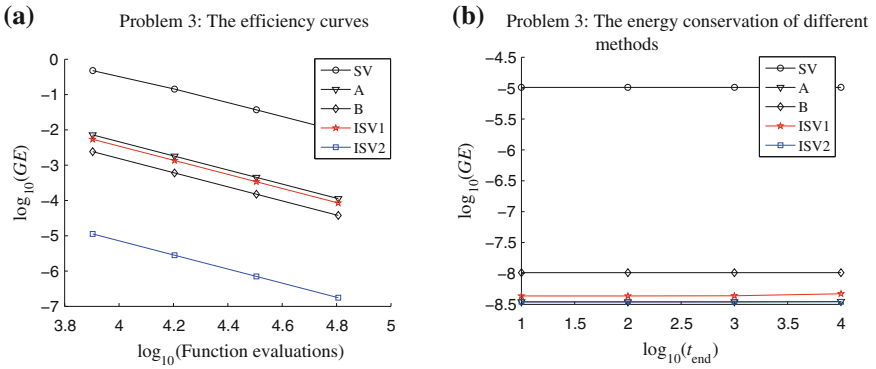

Fig. 2.6 Results for Problem 2.3. **a** The logarithm of the global error (GE) over the integration interval against the logarithm of the number of function evaluations. **b** The logarithm of the maximum global error of Hamiltonian $GEH = \max |H_n - H_0|$ against $\log_{10}(t_{\text{end}})$

where q_1 stands for the radial displacement of the orbit of a star from a reference circular orbit, and q_2 stands for the deviation of the orbit from the galactic plane. The time variable t actually denotes the angle of the planets in a reference coordinate system. Following [1], we choose $a = 2,\ b = 1$. The problem has been solved on the interval [0, 1000] with $\varepsilon = 10^{-3}$. The stepsizes are taken as $h = 1/(2^j)$ with $j = 3, \ldots, 6$. The numerical results are shown in Fig. 2.7a.

It is easy to see that this system is a Hamiltonian system with the Hamiltonian

$$H = \frac{1}{2}(p_1^2 + p_2^2) + \frac{1}{2}(4q_1^2 + q_2^2) - \varepsilon q_1 q_2^2.$$

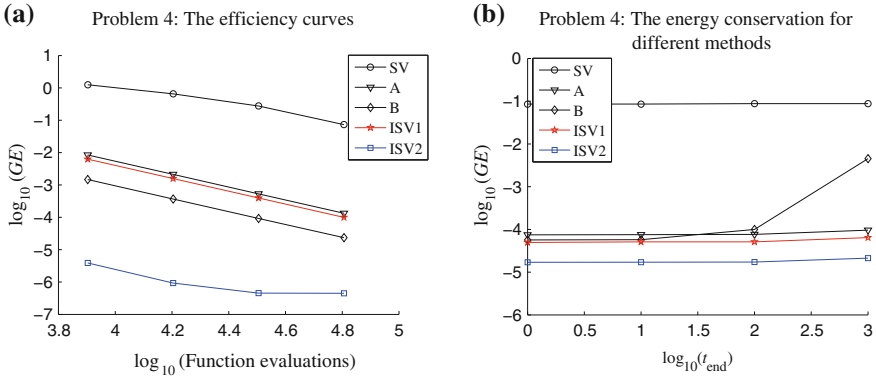

Fig. 2.7 Results for Problem 2.4. **a** The logarithm of the global error (GE) over the integration interval against the logarithm of the number of function evaluations. **b** The logarithm of the maximum global error of Hamiltonian $GEH = \max |H_n - H_0|$ against $\log_{10}(t_{\text{end}})$

Accordingly, we integrate this problem with the stepsize $h = 1/5$ on the interval $[0, 10^i]$, $i = 0, 1, 2, 3$. The energy conservation for different methods is shown in Fig. 2.7b.

2.4.4 Application 4: Fermi–Pasta–Ulam Problem

The Fermi–Pasta–Ulam problem is an important model of non-linear classical and quantum systems of interacting particles in the physics of non-linear phenomena.

Problem 2.5 The Fermi–Pasta–Ulam problem discussed by Hairer et al. [16, 19]. The motion is described by a Hamiltonian system with the total energy

$$H(p, q) = \frac{1}{2} p^{\intercal} p + \frac{1}{2} q^{\intercal} M q + U(q),$$

where

$$M = \begin{pmatrix} \mathbf{0}_{m\times m} & \mathbf{0}_{m\times m} \\ \mathbf{0}_{m\times m} & \omega^2 I_{m\times m} \end{pmatrix},$$

$$U(q) = \frac{1}{4}\left((q_1 - q_{m+1})^4 + \sum_{i=1}^{m-1} (q_{i+1} - q_{m+i+1} - q_i - q_{m+i})^4 + (q_m + q_{2m})^4 \right).$$

Here, q_i represents a scaled displacement of the ith stiff spring, q_{m+i} is a scaled expansion (or compression) of the ith stiff spring, and p_i and p_{m+i} are their velocities (or momenta).

The corresponding Hamiltonian system now becomes

$$\begin{cases} p'(t) = -H_q\big(p(t), q(t)\big), \\ q'(t) = H_p\big(p(t), q(t)\big), \end{cases}$$

which is identical to $q''(t) = -H_q\big(p(t), q(t)\big)$ with $p(t) = q'(t)$. Then we have

$$q''(t) + Mq(t) = -\nabla U\big(q(t)\big), \qquad t \in [t_0, t_{\text{end}}],$$

Following Hairer et al. [19], we consider $m = 3$, and choose

$$q_1(0) = 1,\ p_1(0) = 1,\ q_4(0) = \frac{1}{\omega},\ p_4(0) = 1,$$

with zero for the remaining initial values. The system is integrated on the interval $[0, 10]$ with the stepsizes $h = 0.01/2^j$, $j = 2, \ldots, 5$ for $\omega = 100$ and 200. The results are shown in Fig. 2.8. In Fig. 2.8b, the error $\log_{10}(GE)$ for SV method is very large when $\omega = 200$ and $h = 0.01$, hence the point is not plotted in the graph. For

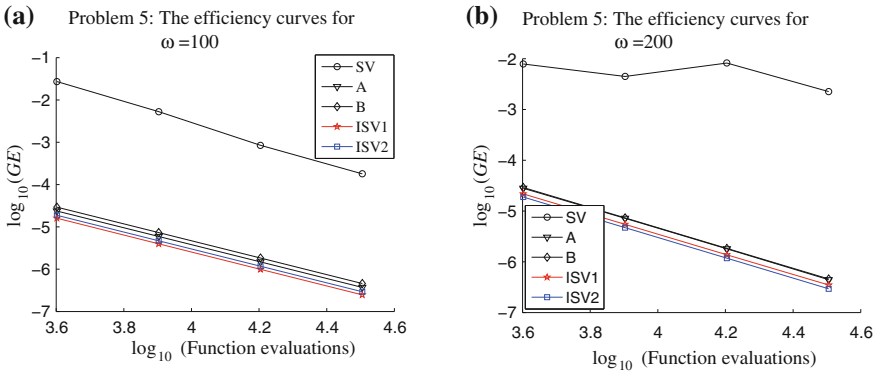

Fig. 2.8 Results for Problem 2.5 with different ω. The logarithm of the global error (GE) over the integration interval against the logarithm of the number of function evaluations

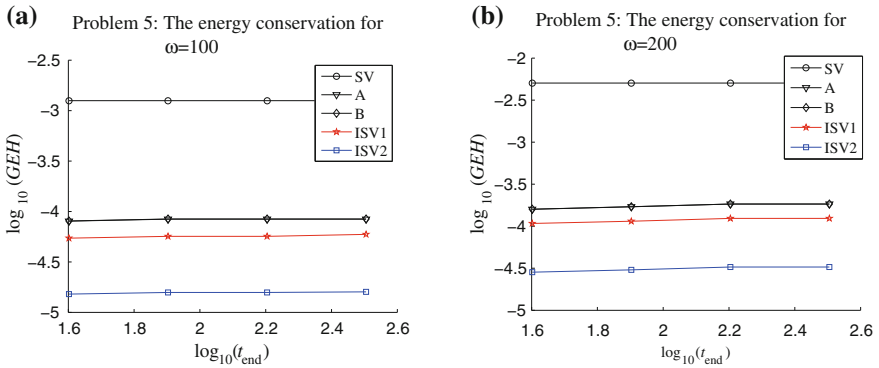

Fig. 2.9 Results for Problem 2.5 with different ω. The logarithm of the maximum global error of Hamiltonian $GEH = \max |H_n - H_0|$ against $\log_{10}(t_{\text{end}})$

global errors of Hamiltonian, this problem is integrated with the stepsize $h = 0.001$ on the intervals $[0, 2^i \times 10]$, $i = 2, \ldots, 5$. The results for different $\omega = 100$ and 200 are shown in Fig. 2.9.

For this Hamiltonian problem, long time-step methods may lead to the problem of numerically induced resonance instabilities. Here, in order to discuss the resonance instabilities for this Hamiltonian problem, we compute the maximum global error of the total energy H as a function of the scaled frequency $h\omega$ (stepsize $h = 0.02$). We consider the long-time interval $[0, 1000]$. Figures 2.10 and 2.11 present the results of the different methods. Method SV shows a poor energy conservation when $h\omega$ is more than about $\pi/2$, while methods ISV1 and ISV2 do poorly only near integral multiples of π. Method A shows poor energy conservation near even multiples of π and only the method B shows a uniformly good behaviour for all frequencies.

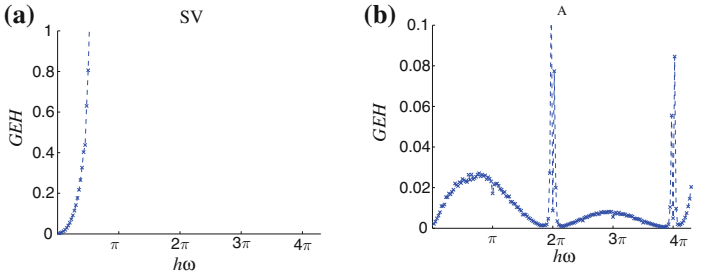

Fig. 2.10 Results for Problem 2.5. The maximum global error (GEH) of the total energy on the interval [0, 1000] for methods SV (*left*), and A (*right*) as a function of $h\omega$ (step size $h = 0.02$)

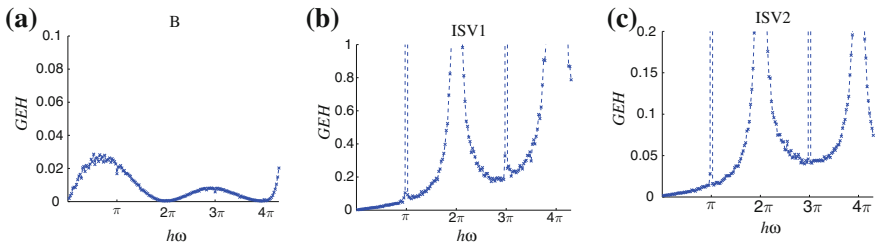

Fig. 2.11 Results for Problem 2.5. The maximum global error (GEH) of the total energy on the interval [0, 1000] for methods B (*left*), ISV1 (*middle*) and ISV2 (*right*) as a function of $h\omega$ (step size $h = 0.02$)

From the numerical results of the four types of problems, it follows that the two improved multidimensional Störmer–Verlet formulae show better accuracy and preserve the Hamiltonian approximately better than the classical Störmer–Verlet formula (2.4) and the two Gautschi-type methods A and B. It is noted that the formula ISV2 behaves better than the formula ISV1. The reason for this numerical behaviour is that the formula ISV2 uses the special structure brought by the linear term My from the problem (2.1) not only in the updates but also in the internal stages, whereas the formula ISV1 uses the special structure only in the updates. In other words, the numerical behaviour of the two improved formulae shows the importance and the superiority of using special structure to obtain structure-preserving algorithms.

2.5 Coupled Conditions for Explicit Symplectic and Symmetric Multi-frequency ERKN Integrators for Multi-frequency Oscillatory Hamiltonian Systems

It can be verified that the symplectic improved Störmer–Verlet formulae ISV2 is also symmetric. Therefore, this section pays attention to the coupled conditions for symplectic and symmetric multi-frequency extended Runge-Kutta-Nyström integrators (SSMERKN) for multi-frequency and multidimensional oscillatory Hamiltonian

systems with the Hamiltonian $H(p,q) = p^{\intercal}p/2 + q^{\intercal}Aq/2 + U(q)$, where A is a symmetric and positive semi-definite matrix implicitly preserving the dominant frequencies of the oscillatory problem, and $U(q)$ is a real-valued function with continuous second derivatives. The solution of the system is a non-linear multi-frequency oscillator. The coupled conditions are presented for SSMERKN integrators. When $A = \mathbf{0} \in \mathbb{R}^{d\times d}$, the explicit SSMERKN integrators reduce to classical symplectic and symmetric RKN methods.

2.5.1 *Towards Coupled Conditions for Explicit Symplectic and Symmetric Multi-frequency ERKN Integrators*

This section turns to the coupled conditions for symplectic and symmetric multi-frequency ERKN integrators (SSMERKN) for multi-frequency and multidimensional oscillatory Hamiltonian systems

$$\begin{cases} p' = -\nabla_q H(p,q), & p(t_0) = p_0, \\ q' = \nabla_p H(p,q), & q(t_0) = q_0, \end{cases} \tag{2.26}$$

with the Hamiltonian $H(p,q) = p^{\intercal}p/2 + q^{\intercal}Aq/2 + U(q)$, where A is a symmetric and positive semi-definite matrix implicitly preserving the dominant frequencies of the oscillatory problem, and $U(q)$ is a real-valued function with continuous second derivatives. Clearly, if $f(q) = -\nabla U(q)$, then (2.26) is identical to the multi-frequency and multidimensional oscillatory system of second-order differential equations

$$\begin{cases} q''(t) + Aq(t) = f\big(q(t)\big), \\ q(t_0) = q_0, \quad q'(t_0) = q_0'. \end{cases} \tag{2.27}$$

It is important to observe that the system (2.27) is a *multi-frequency and multidimensional oscillatory problem with multiple time scales*.

A significant amount of early work on the numerical integration of (2.27) focused mainly on the *single-frequency problem, the so-called perturbed oscillator*

$$\begin{cases} q''(t) + \omega^2 q(t) = f\big(q(t)\big), & t \in [t_0, T], \\ q(t_0) = q_0, \quad q'(t_0) = q_0', \end{cases} \tag{2.28}$$

where $\omega > 0$ is the *main frequency of the single-frequency problem* and ω may be known or accurately estimated in advance, and $f(q)$ is a small perturbing force. It is clear that (2.28) is a special case of (2.27). Over the past ten years (and earlier), some

novel approaches to modifying classical RKN methods have been proposed for the single-frequency problem (2.28). Franco [10] took advantage of the special structure of (2.28) introduced by the linear term $\omega^2 q$ and modified the updates of classical RKN methods to obtain ARKN methods. For further research following [10], readers are referred to [60, 63]. Also note that Tocino and Vigo-Aguiar [45] presented the symplecticity conditions of modified RKN methods, and Chen et al. [4] gave symmetric and symplectic conditions of ERKN methods for the *single-frequency problem* (2.28). All the methods designed specially for the single-frequency problem (2.28) have coefficients which are analytic functions of ν^2 ($\nu = h\omega$). It is very important to note that, in general, *these methods for the single-frequency problem* (2.28) *cannot be applied to the multi-frequency oscillatory system* (2.27). This fact can be shown by the following Hamiltonian system with the Hamiltonian [25, 26]

$$H = \frac{1}{2}p^{\intercal}p + \frac{1}{2}q^{\intercal}\begin{pmatrix} 4 & 0 \\ 0 & 1 \end{pmatrix} q - \varepsilon q_1 q_2^2. \tag{2.29}$$

The problem (2.29) has two coupled oscillators with two different frequencies. However, it is clear that the coefficients of the methods for single-frequency problems (2.28) are functions of $\nu = h\omega$. Hence the analysis for single-frequency problems (2.28) given in previous publications is not directly applicable to coupled oscillators. Moreover, it has been shown in [59] that a symplectic multi-frequency method requires more coupled conditions than a symplectic single-frequency method, which demonstrates the difference of symplecticity conditions for these two different kinds of methods. Therefore, this section is devoted to developing the coupled conditions of multi-frequency ERKN methods for multi-frequency and multidimensional oscillatory Hamiltonian systems (2.27).

2.5.2 *The Analysis of Combined Conditions for SSMERKN Integrators for Multi-frequency and Multidimensional Oscillatory Hamiltonian Systems*

Many physical problems have time reversibility and this structure of the original continuous system is preserved by symmetric integrators (for a rigorous definition of reversibility readers are referred to Chap. 5 of Hairer et al. [19]). On the other hand, some real-physical processes with negligible dissipation in applications could be modelled by the Hamiltonian system (2.27). The solution of the system preserves the Hamiltonian $H(p, q)$. Furthermore, the corresponding flow is symplectic in the sense that the differential 2-form $\mathrm{d}p \wedge \mathrm{d}q$ is invariant. The important property of symplecticity is preserved by symplectic integrators.

Pioneering work on symplectic integrators is due to [6, 7, 35]. The symplecticity conditions for Runge-Kutta methods are obtained in [37], the symplecticity conditions for RKN methods are derived in [43], and the symplecticity conditions

for multi-frequency ERKN methods are given in [59]. This section is devoted to deriving the coupled conditions of SSMERKN integrators for the multi-frequency and multidimensional oscillatory Hamiltonian system (2.27).

It is noted that explicit integrators do not require the solution of large and complicated systems of non-linear algebraic or transcendental equations when solving the multi-frequency and multidimensional oscillatory problem (2.27). Therefore, this section pays attention only to explicit SSMERKN integrators for (2.27).

The next theorem gives the coupled conditions of explicit SSMERKN integrators for (2.27).

Theorem 2.3 *An s-stage explicit multi-frequency ERKN integrator for integrating (2.27) is symplectic and symmetric if its coefficients are:*

$$\begin{cases} c_i = 1 - c_{s+1-i}, \quad d_i = d_{s+1-i} \neq 0, & i = 1, 2, \ldots, s, \\ b_i(V) = d_i \phi_0(c_{s+1-i}^2 V), & i = 1, 2, \ldots, s, \\ \\ \bar{b}_i(V) = d_i c_{s+1-i} \phi_1(c_{s+1-i}^2 V), & i = 1, 2, \ldots, s, \\ \bar{a}_{ij}(V) = \dfrac{1}{d_i}\big(b_i(V)\bar{b}_j(V) - \bar{b}_i(V) b_j(V)\big), & i > j, \ \ i, \ j = 1, 2, \ldots, s. \end{cases} \tag{2.30}$$

Proof Consider first the symplecticity.

It follows from the symplecticity conditions in [58, 59] that an s-stage explicit multi-frequency ERKN integrator for (2.27) is symplectic if its coefficients satisfy

$$\begin{cases} b_i(V)\phi_0(V) + \bar{b}_i(V) V \phi_1(V) = d_i \phi_0(c_i^2 V), & i = 1, 2, \ldots, s, \quad d_i \in \mathbb{R}, \\ \bar{b}_i(V)\big(\phi_0(V) + c_i V \phi_1(V)\phi_0^{-1}(c_i^2 V)\phi_1(c_i^2 V)\big) \\ \quad = b_i(V)\big(\phi_1(V) - c_i \phi_0(V)\phi_0^{-1}(c_i^2 V)\phi_1(c_i^2 V)\big), & i = 1, 2, \ldots, s, \\ b_i(V)\big(\bar{b}_j(V) - \phi_0(V)\phi_0^{-1}(c_i^2 V)\bar{a}_{ij}(V)\big) - \bar{b}_i(V) V \phi_1(V)\phi_0^{-1}(c_i^2 V)\bar{a}_{ij}(V) \\ \quad = b_j(V)\bar{b}_i(V), & i > j, \ \ i, \ j = 1, 2, \ldots, s. \end{cases} \tag{2.31}$$

With the definition (1.7), a careful calculation shows that

$$\begin{cases} \phi_0(V)\phi_0(c_i^2 V) + c_i V \phi_1(V)\phi_1(c_i^2 V) = \phi_0\big((1 - c_i)^2 V\big) = \phi_0(c_{s+1-i}^2 V), \\ \phi_1(V)\phi_0(c_i^2 V) - c_i \phi_0(V)\phi_1(c_i^2 V) = (1 - c_i)\phi_1\big((1 - c_i)^2 V\big) = c_{s+1-i}\phi_1(c_{s+1-i}^2 V). \end{cases} \tag{2.32}$$

Solving all the symplecticity conditions (2.31) with $d_i \neq 0$ yields

$$\begin{cases} b_i(V) = d_i\big(\phi_0(V)\phi_0(c_i^2 V) + c_i V \phi_1(V)\phi_1(c_i^2 V)\big), & i = 1, 2, \ldots, s, \\ \bar{b}_i(V) = d_i\big(\phi_1(V)\phi_0(c_i^2 V) - c_i \phi_0(V)\phi_1(c_i^2 V)\big), & i = 1, 2, \ldots, s, \\ \bar{a}_{ij}(V) = \dfrac{1}{d_i}\big(b_i(V)\bar{b}_j(V) - \bar{b}_i(V) b_j(V)\big), & i > j, \ \ i, \ j = 1, 2, \ldots, s. \end{cases} \tag{2.33}$$

The formulae (2.32) and (2.33) immediately show that the coefficients $b_i(V)$, $\bar{b}_i(V)$, $\bar{a}_{ij}(V)$ in (2.30) satisfy the symplecticity conditions (2.31) for s-stage explicit multi-frequency ERKN integrators.

The purpose of the next step is to verify that the explicit multi-frequency ERKN integrator given by (2.30) is symmetric.

It is known that an integrator $y_{n+1} = \Phi_h(y_n)$ is symmetric if exchanging $y_n \leftrightarrow y_{n+1}$ and $h \leftrightarrow -h$ does not change the integrator. Hence, exchanging $(q_n, p_n) \leftrightarrow (q_{n+1}, p_{n+1})$ and replacing h by $-h$ for an s-stage explicit multi-frequency ERKN method gives

$$\begin{cases} \hat{Q}_i = \phi_0(c_i^2V)q_{n+1} - hc_i\phi_1(c_i^2V)p_{n+1} + h^2\sum\limits_{j=1}^{i-1}\bar{a}_{ij}(V)\big(-\nabla U(\hat{Q}_j)\big), \quad i = 1, 2, \ldots, s, \\ q_n = \phi_0(V)q_{n+1} - h\phi_1(V)p_{n+1} + h^2\sum\limits_{i=1}^{s}\bar{b}_i(V)\big(-\nabla U(\hat{Q}_i)\big), \\ p_n = hA\phi_1(V)q_{n+1} + \phi_0(V)p_{n+1} - h\sum\limits_{i=1}^{s}b_i(V)\big(-\nabla U(\hat{Q}_i)\big). \end{cases} \tag{2.34}$$

It follows from (2.34) that

$$\begin{cases} \hat{Q}_i = \phi_0((1-c_i)^2V)q_n + h(1-c_i)\phi_1((1-c_i)^2V)p_n + h^2\sum\limits_{j=1}^{i-1}\big[\phi_0(c_i^2V)\big(\phi_1(V)b_j(V) \\ \qquad - \phi_0(V)\bar{b}_j(V)\big) - c_i\phi_1(c_i^2V)\big(V\phi_1(V)\bar{b}_j(V) + \phi_0(V)b_j(V)\big) + \bar{a}_{ij}(V)\big]\big(-\nabla U(\hat{Q}_j)\big), \\ q_{n+1} = \phi_0(V)q_n + h\phi_1(V)p_n + h^2\sum\limits_{i=1}^{s}\big[\phi_1(V)b_i(V) - \phi_0(V)\bar{b}_i(V)\big]\big(-\nabla U(\hat{Q}_i)\big), \\ p_{n+1} = -hA\phi_1(V)q_n + \phi_0(V)p_n + h\sum\limits_{i=1}^{s}\big[V\phi_1(V)\bar{b}_i(V) + \phi_0(V)b_i(V)\big]\big(-\nabla U(\hat{Q}_i)\big). \end{cases} \tag{2.35}$$

Replacing all indices i and j in (2.35) by $s+1-i$ and $s+1-j$, respectively, it is easy to see that an s-stage explicit multi-frequency ERKN method is symmetric if the following conditions are true:

$$\begin{cases} c_i = 1 - c_{s+1-i}, & i = 1, 2, \ldots, s, \\ \bar{b}_i(V) = \phi_1(V)b_{s+1-i}(V) - \phi_0(V)\bar{b}_{s+1-i}(V), & i = 1, 2, \ldots, s, \\ b_i(V) = V\phi_1(V)\bar{b}_{s+1-i}(V) + \phi_0(V)b_{s+1-i}(V), & i = 1, 2, \ldots, s, \\ \bar{a}_{ij}(V) = \phi_0(c_{s+1-i}^2V)\bar{b}_j(V) - c_{s+1-i}\phi_1(c_{s+1-i}^2V)b_j(V), & i > j, \ \ i, \ j = 1, 2, \ldots, s. \end{cases} \tag{2.36}$$

It follows from (2.30) and (1.7) that

$$\begin{aligned} \phi_1(V)b_{s+1-i}(V) - \phi_0(V)\bar{b}_{s+1-i}(V) &= d_{s+1-i}c_{s+1-i}\phi_1(c_{s+1-i}^2V) \\ &= d_ic_{s+1-i}\phi_1(c_{s+1-i}^2V) = \bar{b}_i(V), \ i = 1, 2, \ldots, s, \\ V\phi_1(V)\bar{b}_{s+1-i}(V) + \phi_0(V)b_{s+1-i}(V) &= d_{s+1-i}\phi_0(c_{s+1-i}^2V) \\ &= d_i\phi_0(c_{s+1-i}^2V) = b_i(V), \ i = 1, 2, \ldots, s, \end{aligned}$$

and

$$\begin{aligned}\bar{a}_{ij}(V) &= \frac{1}{d_i}\big(b_i(V)\bar{b}_j(V) - \bar{b}_i(V)b_j(V)\big)\\ &= \phi_0(c_{s+1-i}^2 V)\bar{b}_j(V) - c_{s+1-i}\phi_1(c_{s+1-i}^2 V)b_j(V), \quad i > j, \quad i,\ j = 1, 2, \ldots, s.\end{aligned}$$

This means that an s-stage explicit multi-frequency ERKN integrator with the coefficients (2.30) is symplectic and symmetric. This completes the proof. □

Remark 2.1 It follows from Theorem 2.3 that the coefficients (2.30) are expressed by c_i, d_i, $\phi_0(V)$ and $\phi_1(V)$. In order to compute matrix-valued functions $\phi_0(V)$ and $\phi_1(V)$, recall that a *generalized hypergeometric function* (see [32, 39]) is

$$ {}_mF_n\left[\begin{matrix}\alpha_1, \alpha_2, \ldots, \alpha_m;\\ \beta_1, \beta_2, \ldots, \beta_n;\end{matrix} x\right] = \sum_{l=0}^{\infty} \frac{\prod_{i=1}^{m}(\alpha_i)_l}{\prod_{i=1}^{n}(\beta_i)_l}\frac{x^l}{l!}, \tag{2.37}$$

where the *Pochhammer symbol* $(z)_l$ is defined as $(z)_0 = 1$ and $(z)_l = z(z+1)\cdots(z+l-1)$, $l \in \mathbb{N}$. The parameters α_i and β_i are arbitrary complex numbers, except that β_i can be neither zero nor a negative integer. It is noted that $\phi_0(V)$ and $\phi_1(V)$ can be expressed by the generalized hypergeometric function ${}_0F_1$:

$$\phi_0(V) = {}_0F_1\left[\begin{matrix}-;\\ \frac{1}{2};\end{matrix} -\frac{V}{4}\right], \quad \phi_1(V) = {}_0F_1\left[\begin{matrix}-;\\ \frac{3}{2};\end{matrix} -\frac{V}{4}\right]. \tag{2.38}$$

Most modern software, e.g. Maple, Mathematica, or Matlab, is well equipped to calculate generalized hypergeometric functions, and there is also much work concerning the evaluation of generalized hypergeometric functions of a matrix argument (see, e.g. [2, 15, 22, 27, 33]). Moreover, there have been some efficient ways to compute the matrix cosine and sine, and readers are referred to [21, 22, 31, 36] for example. All these publications provide different ways to deal with the computation of $\phi_0(V)$ and $\phi_1(V)$.

It is noted that when $V \to \mathbf{0}_{d\times d}$, the multi-frequency ERKN methods reduce to classical RKN methods for solving Hamiltonian systems with the Hamiltonian $H(p,q) = \frac{1}{2}p^{\intercal}p + U(q)$. The following result can be obtained from Theorem 2.3.

Theorem 2.4 *An s-stage explicit RKN method with the coefficients*

$$\begin{cases} c_i = 1 - c_{s+1-i}, \quad d_i = d_{s+1-i} \neq 0, & i = 1, 2, \ldots, s,\\ b_i = d_i, \quad \bar{b}_i = d_i c_{s+1-i}, & i = 1, 2, \ldots, s,\\ \bar{a}_{ij} = \frac{1}{d_i}\big(b_i\bar{b}_j - \bar{b}_i b_j\big), & i > j, \quad i,\ j = 1, 2, \ldots, s, \end{cases} \tag{2.39}$$

is symplectic and symmetric. In (2.39), $d_i,\ i = 1, 2, \ldots, \lfloor \frac{s+1}{2} \rfloor$, *are real numbers and can be chosen according to the order conditions of RKN methods or other ways, where* $\lfloor \frac{s+1}{2} \rfloor$ *denotes the integral part of* $\frac{s+1}{2}$.

Proof It follows from (2.39) that

$$\begin{aligned}
&\bar{b}_i = d_i c_{s+1-i} = b_i(1 - c_i), && i = 1, 2, \ldots, s,\\
&b_i(\bar{b}_j - \bar{a}_{ij}) = b_i\Big(\bar{b}_j - \frac{1}{d_i}(b_i\bar{b}_j - \bar{b}_i b_j)\Big)\\
&= b_i(\bar{b}_j - \bar{b}_j) + \bar{b}_i b_j = \bar{b}_i b_j, && i > j,\ \ i,\ j = 1, 2, \ldots, s,
\end{aligned}$$

which are exactly the symplecticity conditions for explicit RKN methods.

Moreover, based on (2.39), we have

$$\begin{aligned}
&c_i = 1 - c_{s+1-i}, \quad b_i = d_i = d_{s+1-i} = b_{s+1-i}, \quad i = 1, 2, \ldots, s,\\
&\bar{a}_{ij} = \frac{1}{d_i}(b_i\bar{b}_j - \bar{b}_i b_j) = \frac{1}{d_i}(d_i\bar{b}_j - d_i c_{s+1-i} b_j)\\
&= \bar{b}_j - c_{s+1-i} b_j, && i > j,\ \ i,\ j = 1, 2, \ldots, s,
\end{aligned}$$

and these are the symmetry conditions for explicit RKN methods. The proof is complete. □

2.6 Conclusions and Discussions

The well-known Störmer–Verlet formula can be implemented easily, and it has become by far the most widely used numerical scheme. This chapter develops two improved Störmer–Verlet formulae ISV1 and ISV2 by exploiting the special structure of the problem (2.1). The two improved formulae are shown to be symplectic schemes of order two and are generalizations of the classical Störmer–Verlet scheme since when $M \to \mathbf{0}_{d\times d}$, they reduce to the classical Störmer–Verlet formula (2.4). It is known that the advantage of symplectic algorithms is that they show a sort of global stability. Each improved method is a blend of existing trigonometric integrators and symplectic integrators, fully combining the favourable properties of both. Based on the linear test Eq. (2.21), the stability and phase properties for the two improved Störmer–Verlet formulae are also analysed. In order to exhibit the two formulae quantitatively, four different applications, including time-independent Schrödinger equations, non-linear wave equations, orbital problems and the Fermi-Pasta-Ulam problem, are presented. The two improved formulae are compared with the classical Störmer–Verlet formula and the two other improved Störmer–Verlet methods that have appeared already in the literature. The numerical experiments recorded in this chapter demonstrate that the improved Störmer–Verlet formulae are more efficient than the classical Störmer–Verlet formula, and the two other methods that have already appeared in the literature. In particular, it can be concluded

that, when applied to a Hamiltonian system, the two improved Störmer–Verlet formulae preserve well the Hamiltonian in the sense of numerical approximation and have better accuracy than those of the classical Störmer–Verlet formula and the two Gautschi-type methods A and B with the same computational cost.

Since the improved Störmer–Verlet formula ISV2 is an explicit symplectic and symmetric multi-frequency ERKN integrator for multi-frequency oscillatory Hamiltonian systems, the coupled conditions for explicit symplectic and symmetric multi-frequency ERKN integrators for multi-frequency oscillatory Hamiltonian systems are investigated in detail.

Last but not least, like the classical Störmer–Verlet formula (2.4), it can be observed clearly that the two improved Störmer–Verlet formulae ISV1 given by (2.15) and ISV2 given by (2.20) are conceptually simple, versatile and easy to code when applied to (2.1) or (2.2). It seems promising that, for the two improved Störmer–Verlet formulae ISV1 and ISV2, other applications may be found in science and engineering.

This chapter is based on the work by Wang et al. [54], and a seminar report by Wang and Wu [52].

References

1. Ariel G, Engquist B, Kim S, Lee Y, Tsai R (2013) A multiscale method for highly oscillatory dynamical systems using a Poincaré map type technique. J Sci Comput 54:247–268
2. Butler RW, Wood ATA (2002) Laplace approximations for hypergeometric functions with matrix argument. Ann Statist 30:1155–1177
3. Candy J, Rozmus W (1991) A symplectic integration algorithm for separable Hamiltonian functions. J Comput Phys 92:230–256
4. Chen Z, You X, Shi W, Liu Z (2012) Symmetric and symplectic ERNK methods for oscillatory Hamiltonian systems. Comput Phys Commun 183:86–98
5. Cohen D, Jahnke T, Lorenz K, Lubich C (2006) Numerical integrators for highly oscillatory Hamiltonian systems: a review. In: Mielke A (ed) Analysis, modeling and simulation of multiscale problems. Springer, Berlin, pp 553–576
6. De Vogelaere R (1956) Methods of integration which preserve the contact transformation property of the Hamiltonian equations. Report No. 4, Department of Mathematics, University of Notre Dame, Notre Dame, Indiana
7. Feng K (1985) On difference schemes and symplectic geometry. In: Proceedings of the 5th international symposium on differential geometry and differential equations, Beijing, 42–58 Aug 1984
8. Feng K, Qin M (2010) Symplectic geometric algorithms for hamiltonian systems. Springer, Berlin
9. Fermi E, Pasta J, Ulam S (1955) Studies of the Nonlinear Problems, I. Los Alamos Report No. LA- 1940, later published in E. Fermi: Collected Papers (Chicago 1965), and Lect Appl Math 15:143 (1974)
10. Franco JM (2002) Runge-Kutta-Nyström methods adapted to the numerical integration of perturbed oscillators. Comput Phys Commun 147:770–787
11. Franco JM (2006) New methods for oscillatory systems based on ARKN methods. Appl Numer Math 56:1040–1053
12. García A, Martín P, González AB (2002) New methods for oscillatory problems based on classical codes. Appl Numer Math 42:141–157

13. García-Archilla B, Sanz-Serna JM, Skeel RD (1999) Long-time-step methods for oscillatory differential equations. SIAM J Sci Comput 20:930–963
14. González AB, Martín P, Farto JM (1999) A new family of Runge-Kutta type methods for the numerical integration of perturbed oscillators. Numer Math 82:635–646
15. Gutiérrez R, Rodriguez J, Sáez AJ (2000) Approximation of hypergeometric functions with matricial argument through their development in series of zonal polynomials. Electron Trans Numer Anal 11:121–130
16. Hairer E, Lubich C (2000) Long-time energy conservation of numerical methods for oscillatory differential equations. SIAM J Numer Anal 38:414–441
17. Hairer E, Lubich C, Wanner G (2003) Geometric numerical integration illustrated by the Störmer-Verlet method. Acta Numerica 12:399–450
18. Hairer E, Lubich C (2000) Energy conservation by Störmer-type numerical integrators. In: Griffiths GF, Watson GA (eds) Numerical analysis 1999. CRC Press LLC, pp 169–190
19. Hairer E, Lubich C, Wanner G (2006) Geometric numerical integration: structure-preserving algorithms for ordinary differential equations, 2nd edn. Springer, Berlin
20. Hairer E, Nørsett SP, Wanner G (1993) Solving ordinary differential equations I: nonstiff problems. Springer, Berlin
21. Hargreaves GI, Higham NJ (2005) Efficient algorithms for the matrix cosine and sine. Numer Algo 40:383–400
22. Higham NJ, Smith MI (2003) Computing the matrix cosine. Numer Algo 34:13–26
23. Hochbruck M, Lubich C (1999) A Gautschi-type method for oscillatory second-order differential equations. Numer Math 83:403–426
24. Kalogiratou Z, Monovasilis Th, Simos TE (2003) Symplectic integrators for the numerical solution of the Schrödinger equation. J Comput Appl Math 158:83–92
25. Kevorkian J, Cole JD (1981) Perturbation methods in applied mathematics. Applied mathematical sciences, vol 34, Springer, New York
26. Kevorkian J, Cole JD (1996) Multiple scale and singular perturbation methods. Applied mathematical sciences, vol 114, Springer, New York
27. Koev P, Edelman A (2006) The efficient evaluation of the hypergeometric function of a matrix argument. Math Comput 75:833–846
28. Li J, Wang B, You X, Wu X (2011) Two-step extended RKN methods for oscillatory systems. Comput Phys Commun 182:2486–2507
29. Li J, Wu X (2013) Adapted Falkner-type methods solving oscillatory second-order differential equations. Numer Algo 62:355–381
30. McLachlan RI, Quispel GRW (2002) Splitting methods. Acta Numerica 11:341–434
31. Püschel M, Moura JMF (2003) The algebraic approach to the discrete cosine and sine transforms and their fast algorithms. SIAM J Comput 32:1280–1316
32. Rainville ED (1960) Special functions. Macmillan, New York
33. Richards DSP (2011) High-dimensional random matrices from the classical matrix groups, and generalized hypergeometric functions of matrix argument. Symmetry 3:600–610
34. Rowlands G (1991) A numerical algorithm for Hamiltonian systems. J Comput Phys 97:235–239
35. Ruth RD (1983) A canonical integration technique. IEEE Trans Nucl Sci 30:2669–2671
36. Serbin SM, Blalock SA (1980) An algorithm for computing the matrix cosine. SIAM J Sci Stat Comput 1:198–204
37. Sanz-Serna JM (1988) Runge-Kutta schems for Hamiltonian systems. BIT Numer Math 28:877–883
38. Simos TE (2010) Exponentially and trigonometrically fitted methods for the solution of the Schrödinger equation. Acta Appl Math 110:1331–1352
39. Slater LJ (1966) Generalized hypergeometric functions. Cambridge University Press, Cambridge
40. Stavroyiannis S, Simos TE (2009) Optimization as a function of the phase-lag order of two-step P-stable method for linear periodic IVPs. Appl Numer Math 59:2467–2474
41. Stiefel EL, Scheifele G (1971) Linear and regular celestial mechanics. Springer, New York

42. Störmer C (1907) Sur les trajectories des corpuscules électrisés. Arch Sci Phys Nat 24:5–18, 113–158, 221–247
43. Suris YB (1989) The canonicity of mapping generated by Runge-Kutta type methods when integrating the systems $\ddot{x} = -\frac{\partial U}{\partial x}$. Zh. Vychisl Mat i Mat Fiz 29:202–211. (In Russian) Translation, U.S.S.S. Comput Maths Math Phys 29:138–144 (1989)
44. Tan X (2005) Almost symplectic Runge-Kutta schemes for Hamiltonian systems. J Comput Phys 203:250–273
45. Tocino A, Vigo-Aguiar J (2005) Symplectic conditions for exponential fitting Runge-Kutta-Nyström methods. Math Comput Modell 42:873–876
46. Berghe VG, Van Daele M (2006) Exponentially-fitted Störmer/Verlet methods. JNAIAM J Numer Anal Ind Appl Math 1:241–255
47. Van der Houwen PJ, Sommeijer BP (1987) Explicit Runge-Kutta(-Nyström) methods with reduced phase errors for computing oscillating solution. SIAM J Numer Anal 24:595–617
48. Van de Vyver H (2006) An embedded phase-fitted modified Runge-Kutta method for the numerical integration of the radial Schrödinger equation. Phys Lett A 352:278–285
49. Verlet L (1967) Computer "experiments" on classical fluids. I. Thermodynamical properties of Lennard-Jones molecules. Phys Rev 159:98–103
50. Vigo-Aguiar J, Simos TE (2002) Family of twelve steps exponential fitting symmetric multistep methods for the numerical solution of the Schrödinger equation. J Math Chem 32:257–270
51. Vigo-Aguiar J, Simos TE, Ferrándiz JM (2004) Controlling the error growth in long-term numerical integration of perturbed oscillations in one or more frequencies. Proc Roy Soc London Ser A 460:561–567
52. Wang B, Wu X (2013) Coupled conditions for explicit symplectic and symmetric multi-frequency ERKN integrators. A seminar report of Nanjing University [preprint]
53. Wang B, Wu X (2012) A new high precision energy-preserving integrator for system of oscillatory second-order differential equations. Phys Lett A 376:1185–1190
54. Wang B, Wu X, Zhao H (2013) Novel improved multidimensional Stormer-Verlet formulas with applications to four aspects in scientific computation. Math Comput Model 57:857–872
55. Wu X (2012) A note on stability of multidimensional adapted Runge-Kutta-Nyström methods for oscillatory systems. Appl Math Modell 36:6331–6337
56. Wu X, Wang B (2010) Multidimensional adapted Runge-Kutta-Nyström methods for oscillatory systems. Comput Phys Commun 181:1955–1962
57. Wu X, Wang B, Shi W (2013) Efficient energy-preserving integrators for oscillatory Hamiltonian systems. J Comput Phys 235:587–605
58. Wu X, Wang B, Xia J (2010) ESRKN methods for Hamiltonian Systems. In: Vigo Aguiar J (ed) Proceedings of the 2010 international conference on computational and mathematical methods in science and engineering, Vol III, Spain, pp 1016–1020
59. Wu X, Wang B, Xia J (2012) Explicit symplectic multidimensional exponential fitting modified Runge-Kutta-Nyström methods. BIT Num Math 52:773–795
60. Wu X, You X, Li J (2009) Note on derivation of order conditions for ARKN methods for perturbed oscillators. Comput Phys Commun 180:1545–1549
61. Wu X, You X, Shi W, Wang B (2010) ERKN integrators for systems of oscillatory second-order differential equations. Comput Phys Commun 181:1873–1887
62. Wu X, You X, Wang B (2013) Structure-preserving algorithms for oscillatory differential equations. Springer, Berlin
63. Wu X, You X, Xia J (2009) Order conditions for ARKN methods solving oscillatory systems. Comput Phys Commun 180:2250–2257

http://www.springer.com/978-3-662-48155-4

Structure-Preserving Algorithms for Oscillatory Differential Equations II

Wu, X.; Liu, K.; Shi, W.

2015, XV, 298 p. 55 illus., 11 illus. in color., Hardcover
ISBN: 978-3-662-48155-4